Double Diffusive Nonlinear Convective MHD Unsteady Slip-Flow Regime in a Rectangular Channel

ABDULHAKEEM YUSUF[1,a*], TEMITOPE SAMSON ADEKUNLE[2],
ABD'GAFAR TUNDE TIAMIYU[3], ABUBAKAR MUSA ALIYU[1]
[1]Department of Mathematics,
Federal University of Technology Minna,
P.M.B. 65, Minna,
NIGERIA

[2]Department of Computer and Information Science,
Colorado State University,
Colorado,
USA

[3]Department of Mathematics,
The Chinese University of Hong Kong,
Hong Kong,
CHINA

[a]ORCIDiD: 0000-0001-8675-5137

**Corresponding Author*

Abstract: - In the paper, we numerically explored the combined impacts of non-linear thermal and mixed convective unsteady flow in a channel with slip conditions. The flow is caused by a moving flat parallel surface and is also electrically conductive. We analyse the mechanisms of heat, and mass transfer by incorporating temperature and concentration jumps. To simplify the model problem, we apply appropriate similarity transformations, reducing the prevailing problem to a nonlinear coupled ordinary boundary value problem. The transformed problem is solved using the Chebyshev Collocation Approach (CCA). We performed a comparative analysis by comparing the CCA with the literature to verify the accuracy of our approach, and a good agreement is found. In addition, we conducted a comprehensive parametric study to analyze the trends in the solutions obtained. The study reveals that the parameters M, α_1, α_3, Pr, and Sc have about 20% stronger impact on the nonlinear system compared to the linear system on both surfaces of the horizontal channel.

Key-Words: - Double diffusive, Nonlinear Convection, Slip-flow, Channel flow, MHD, Variable distance, Chebyshev Collocation Approach

Received: December 14, 2022. Revised: October 21, 2023. Accepted: November 16, 2023. Published: December 19, 2023.

1 Introduction

Any fluid, whether liquid or gas used in heating or cooling is an example of heat transfer fluid. Heat transfer fluid has a lot of industrial applications and are distinct ranging from the less complex static design of advanced multi-loop systems. The process by which heat is transferred to a moving fluid via a heated surface is known as convective heat transfer which can be viewed in two ways. The first is the natural convection, also known as free convection

which occurs due to density differences caused by temperature gradient and thus resulting in internal buoyancy. This phenomenon is commonly observed in bioreactors and some jacket designs prone to internal free convection at low flow rates. However, when external devices such as stirrers or pump ensure the flow rate, forced convection is predominant. As described by, [1], combined convection exists if the impact of buoyancy in non-free convection and the impact of forced flow in free convection are prevalent. They play a significant role in the atmospheric boundary layer flow, solar collectors, electronic equipment, and nuclear reactors.

Numerous scientists examined the significance of convection flow via stretching sheets with variable boundary conditions as seen in, [2], [3]. [4], explored the nonlinear flow of thermal boundary over a linear surface. The examination of time-dependent natural convection flow of a Jefferey fluid with a moving surface along with the impact of temperature and velocity was considered, [5]. In their work, [6], carried out a study on generalized Mittag-Leffler via the analytical solution of natural convection flow of Prabhakal fractional Maxwell fluid with Newton heating. The impact of various fluid behaviors of combined convective heat transport with a nonlinear moving sheet was explored by, [7]. The influence of Dufour and Soret on convective viscoelastic fluid flow over a moving surface enclosed in a porous medium was examined in, [8]. In addition, [9], Explored viscoelastic Walter-B combined convective nanofluid through a non-linear vertical plate with various sizes of parameters. [10], scrutinize a 3D study of non-linear convection in a Maxwell nanofluid along a non-linear radiation numerically. A review of thermal boundary conditions of Magnetohydrodynamics (MHD) free convective nanofluid in a square enclosure is reported by, [11]. Various other works on convective heat transfer can be found in, [12], [13], [14], [15], [16], [17], and related literature.

The numerous advantages of convective problems of electrically conducting fluid on a magnetic field have attracted significant attention due to their wide applicability in Geophysics, Plasma physics, Astrophysics, Missile Technology, and more. The application of the MHD principle has also been found in Biology and Medicine. [18], explored the impacts of Magnetohydrodynamics natural convective rotating nanofluid flow with radiation-absorption, Soret, Hall, and ion slip over a semi-infinite permeable surface and constant heat source. In the presence of Hall current, [19], considered water-based nanofluid MHD squeezing flow between parallel disks through a saturated medium. Ion slip influence on unsteady magnetohydrodynamics rotating convective flow has been explored by, [20]. [21], examined magnetohydrodynamics micropolar fluid flow over a curved surface. The work of MHD flow with convection over a vertically oscillating porous wall with constant heat flux is explored by, [22]. With exponential permeable stretching porous surface, [23], reported the study of magnetohydrodynamics convective flow of a nanofluid. For more studies conducted on MHD flow, interested individuals can refer to references, [24], [25], [26], [27], [28], [29], [30], [31], [32].

Due to a recent industrial application regime of slip-flow, researchers in their numbers have developed an interest in it. In this period of modern industrialization, technology, and science, the significance of the slip-flow regime can never be over-emphasized. In practical terms, the velocity of the particle to the boundary no longer has the same values as the surface. The surface particle takes a definite velocity and slips on the plate. This kind of flow is known as slip-flow regime and its impact cannot be neglected. The phenomenon of this flow regime is prevalent in microchannels, nanochannels, and geothermal regions. Moreover, efforts of the slip-flow regime in a channel have been discussed by various authors including, [33], [34], [35], [36], [37], [38].

From the literature available, the current study introduces a novel aspect of incorporating nonlinear mixed convection into the model proposed by [39]. The model assumes a first-order slip, with temperature and concentration jumps. To solve the resulting model, the Chebyshev Collocation Approach (CCA) will be employed to obtain the numerical approximations. The combination of a nonlinear mixed convection, the varying conditions, and concentration represents a new contribution to the existing literature.

2 Mathematical Analysis

Considering 2D unsteady, laminar boundary layer fluid flow in a horizontal rectangular wall with the

horizontal wall at $y=0$ and at a variable distance $y=h(t)$. The first wall is assumed slippery and stretches with velocity u_0, temperature T of T_0, concentration C of C_0 while the upper wall has $\partial u/\partial y=\partial T/\partial y=\partial C/\partial y=0$ and $v=\partial h/\partial t$, at $y=h(t)$.

Following the work of, [39], and, [40], based on the assumption above, the model equation of the problem with nonlinear convection and slip-flow conditions as depicted in Figure 1 written as:

$$\frac{\partial u}{\partial x}+\frac{\partial v}{\partial y}=0, \tag{1}$$

$$\frac{\partial u}{\partial t}+u\frac{\partial u}{\partial x}+v\frac{\partial u}{\partial y}=\upsilon\frac{\partial u^2}{\partial y^2}-\frac{\sigma B^2}{\rho}u+g(\beta_0(T-T_h)+\beta_1(T-T_h)^2+\beta_2(C-C_h)+\beta_3(C-C_h)^2), \tag{2}$$

$$\frac{\partial T}{\partial t}+u\frac{\partial T}{\partial x}+v\frac{\partial T}{\partial y}=\alpha^*\left(\frac{\partial T^2}{\partial y^2}\right), \tag{3}$$

$$\frac{\partial C}{\partial t}+u\frac{\partial C}{\partial x}+v\frac{\partial C}{\partial y}=D_M\left(\frac{\partial C^2}{\partial y^2}\right), \tag{4}$$

$$\left.\begin{aligned} &y=0: u=\frac{bx}{1-\alpha t}+a_1\frac{\partial u}{\partial y}, v=0,\\ &T=T_0+a_2\frac{\partial T}{\partial y}, C=C_0+a_3\frac{\partial C}{\partial y}\\ &y=h(t): \frac{\partial u}{\partial y}=0, v=\frac{\partial h}{\partial t}, \frac{\partial T}{\partial y}=0, \frac{\partial C}{\partial y}=0 \end{aligned}\right\} \tag{5}$$

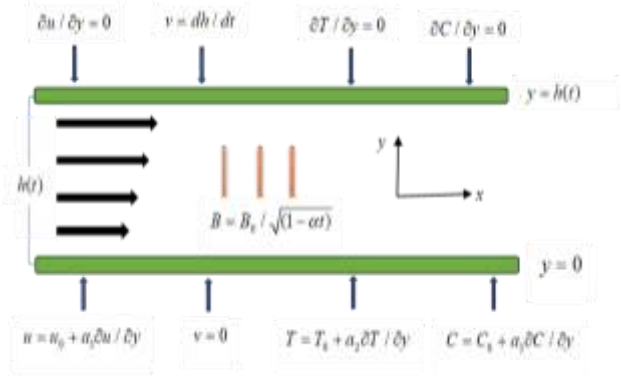

Fig. 1: Model configuration

To simplify the above set of nonlinear partial differential (continuity, momentum, temperature, and concentration profiles) equations (1) – (4) together with the given boundary conditions (5), the following similarity solutions will be used to compact the boundary value problem into a set of non-linear ODEs:

$$\left.\begin{aligned} &\eta=\sqrt{\frac{b}{\upsilon(1-\alpha t)}}\frac{y}{\beta},\quad u=\frac{bx}{1-\alpha t}f'(\eta),\\ &v=-\beta\sqrt{\frac{b\upsilon}{(1-\alpha t)}}f(\eta)\\ &T-T_h=D_1x\theta,\ C-C_h=D_2x\varphi \end{aligned}\right\} \tag{6}$$

The transformed set of nonlinear ordinary equations is:

$$\frac{f'''}{\gamma}-s\frac{\eta}{2}f''+ff''-f'^2-Mf'+\alpha_1\theta(1+\alpha_2\theta)+\alpha_3\varphi(1+\alpha_4\varphi)=0 \tag{7}$$

$$\frac{\theta''}{\gamma\,\mathrm{Pr}}-s\frac{\eta}{2}\theta'-f'\theta+f\theta'=0 \tag{8}$$

$$\frac{\varphi''}{\gamma Sc}-s\frac{\eta}{2}\varphi'-f'\varphi+f\varphi'=0 \tag{9}$$

with the boundary conditions

$$\left.\begin{aligned} &\eta=0: f(0)=0, f'(0)=1+\lambda_1 f''(0),\\ &\theta(0)=1+\lambda_2\theta'(0), \varphi(0)=1+\lambda_3\varphi'(0)\\ &\eta=1: f(1)=\frac{s}{2}, f''(1)=0, \theta'(1)=0, \varphi'(1)=0 \end{aligned}\right\} \tag{10}$$

The critical quantities are the coefficient of skin friction, Nusselt number and Sherwood number obtained as:

$$\frac{\beta C_f}{\sqrt{\mathrm{Re}_x}}=-f''(0), \qquad \frac{\beta Nu_x}{\sqrt{\mathrm{Re}_x}}=-\theta'(0), \qquad \text{and} \qquad \frac{\beta Sh_x}{\sqrt{\mathrm{Re}_x}}=-\varphi'(0)$$

3 Numerical Solution

The reduced nonlinear coupled ODEs corresponding to equations (7)-(10) are solved using the Chebyshev Collocation. This method involves the use of Chebyshev polynomial as basis function by assigning it to an unknown coefficient. The trial function is then implemented on the conditions (Boundary) and the problem of obtaining the residue. Thereby, utilizing a collocation method to generate the error to almost zero. The accuracy of the Colocation technique is found to be high and no ambiguity to implement, [41], [42], [43], [44].

3.1 Chebyshev Collocation Approach Implementation

The functions to be determined $f(\eta)$, $\theta(\eta)$ and $\varphi(\eta)$ are expressed in the form of a sum of Chebyshev base functions below:

$$f(\eta)=\sum_{n=0}^{N}a_nT_n(2\eta-1)\,,\ \theta(\eta)=\sum_{n=0}^{N}b_nT_n(2\eta-1)$$

$$\text{and }\varphi(\eta)=\sum_{n=0}^{N}c_nT_n(2\eta-1)$$

Where a_n, b_n, and c_n are the constants to be determined and $T_n(2\eta-1):[-1,1]\to[0,1]$. In order to obtain the values of the unknown constants, the Chebyshev base functions are substituted into the boundary conditions in (10) corresponding to:

$$\left.\begin{aligned}
&\left[\sum_{n=0}^{N}a_nT_n(2\eta-1)\right]_{\eta=0}=0,\\
&\left[\frac{d}{d\eta}\sum_{n=0}^{N}a_nT_n(2\eta-1)-\frac{d^2}{d\eta^2}\sum_{n=0}^{N}a_nT_n(2\eta-1)-1\right]_{\eta=0}=0,\\
&\left[\sum_{n=0}^{N}b_nT_n(2\eta-1)-\frac{d}{d\eta}\sum_{n=0}^{N}b_nT_n(2\eta-1)-1\right]_{\eta=0}=0,\\
&\left[\sum_{n=0}^{N}c_nT_n(2\eta-1)-\frac{d}{d\eta}\sum_{n=0}^{N}c_nT_n(2\eta-1)-1\right]_{\eta=0}=0,\\
&\left[\frac{d^2}{d\eta^2}\sum_{n=0}^{N}a_nT_n(2\eta-1)=0\right]_{\eta=1}=0,\left[\frac{d}{d\eta}\sum_{n=0}^{N}b_nT_n(2\eta-1)\right]_{\eta=1}=0,\\
&\left[\frac{d}{d\eta}\sum_{n=0}^{N}c_nT_n(2\eta-1)\right]_{\eta=1}=0
\end{aligned}\right\}\quad(11)$$

The base functions are then substituted into equations (7)-(9) to generate the residues $R_f(\eta,a_n,b_n,c_n)$, $R_\theta(\eta,a_n,b_n)$, and $R_\varphi(\eta,a_n,c_n)$. The residues are then minimized using the Collocation techniques as follows:

$$\delta(\eta-\eta_i)=\begin{cases}1, & \eta=\eta_i\\ 0, & \text{otherwise}\end{cases}\quad(12)$$

$$\int_0^L R_f(\eta,a_n,b_n,c_n)d\eta=R_f(\eta,a_n,b_n,c_n)=0,\quad\text{for } i=1,2,3,\ldots N-2\quad(13)$$

$$\int_0^L R_\theta(\eta,a_n,b_n)d\eta=R_f(\eta,a_n,b_n)=0,\quad\text{for } i=1,2,3,\ldots N-1\quad(14)$$

$$\int_0^L R_\varphi(\eta,a_n,c_n)d\eta=R_\varphi(\eta,a_n,c_n)=0,\quad\text{for } i=1,2,3,\ldots N-1\quad(15)$$

Where are the Collocation points expressed as:

$$\eta_i=\frac{1}{2}\left(1-\cos\left(\frac{i\pi}{N}\right)\right),\text{for i=1, 0,…N}\quad(16)$$

Equations (12) to (15) is a 3N+3 x 3N+3 system of equations with unknown coefficients a_n, b_n, and c_n to be obtained.

The corresponding residue equation for equations (7)-(9) is given as:

$$R_1=\frac{f'''}{\gamma}-s\frac{\eta}{2}f''+ff''-f'^2-Mf'+\alpha_1\theta\left(1+\alpha_2\theta\right)+\alpha_3\varphi\left(1+\alpha_4\varphi\right)\quad(17)$$

$$R_2=\frac{\theta''}{\gamma\,\mathrm{Pr}}-s\frac{\eta}{2}\theta'-f'\theta+f\theta'\quad(18)$$

$$R_3=\frac{\varphi''}{\gamma Sc}-s\frac{\eta}{2}\varphi'-f'\varphi+f\varphi'\quad(19)$$

The collocation points are presented in Table. 1 below:

Table 1. Collocation points

i	η_i	i	η_i
0.0	0.000000	10.0	0.578217
1.0	0.006155	11.0	0.654508
2.0	0.054496	12.0	0.726995
3.0	0.095491	13.0	0.793893
4.0	0.146447	14.0	0.853553
5.0	0.206107	15.0	0.904508
6.0	0.273004	16.0	0.945503
7.0	0.345491	17.0	0.975528
8.0	0.421782	18.0	0.993844
9.0	0.500000	19.0	1.000000

Newton's method is employed to obtain the solution of the system and Mathematical symbolic package (MATHEMATICA 11.3) is used to carry out all the computations.

Table 2. Comparison of Nusselt number ($-\theta'(0)$) for $\gamma = 1, M = 0.0, s = 0.0, Sc = 0.1,$ $\alpha_1 = \alpha_2 = \alpha_3 = \alpha_4 = \lambda_1 = \lambda_2 = \lambda_3 = 0$

Pr	[45]	[46]	[47]	Present results
1	1.0000	-	1.0000	1.0008
3	1.9237	-	1.9237	1.9233
6.7	-	3.0002	3.0003	3.0000

4 Results and Discussions

The solution to the highly nonlinear coupled expressions in (7-9) with their conditions in (10) are numerically approximated with the Chebyshev Collocation Method. The implementation of this method has various advantages ranging from the fact that its construction is integration-based as against the traditional differentiation, which allows the incorporation of more than one boundary condition efficiently and faster convergence rate than conventional approaches. To check the accuracy of this method, a comparative analysis is carried out with the literature. An excellent agreement is observed as presented in Table 2.

Figure 2a-2c describe the features of magnetization on f', θ *and* φ respectively for both linear $(\alpha_2 = \alpha_4 = 0)$ and nonlinear $(\alpha_2 \neq 0, \alpha_4 \neq 0)$ combined convection. It is explored that the horizontal velocity f' in Figure 2a retarded for improving M due to the magnetization of the lower wall to help weaken the fluid momentum. Fluid energy θ and concentration φ are escalated in Figure 2b and Figure 2c respectively. The fluid velocities drop faster for linear convection than nonlinear convection and the temperature and concentration enhance faster with linear convection. This phenomenon implies that the Lorentz force has a greater impact on the linear mixed convection compared to the nonlinear.

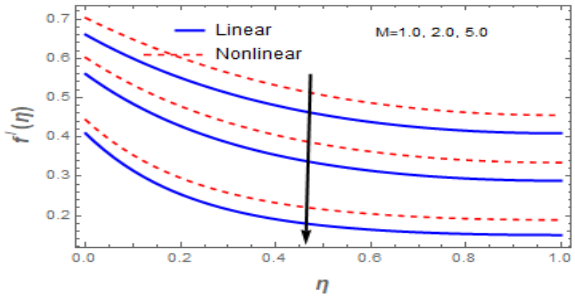

(a)

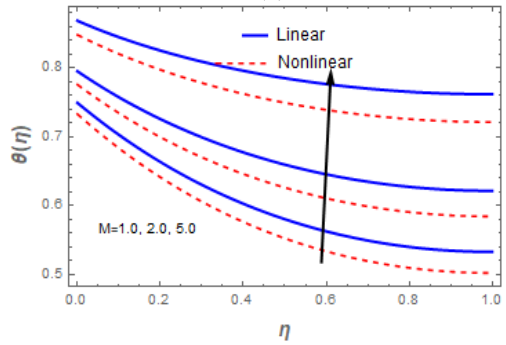

(b)

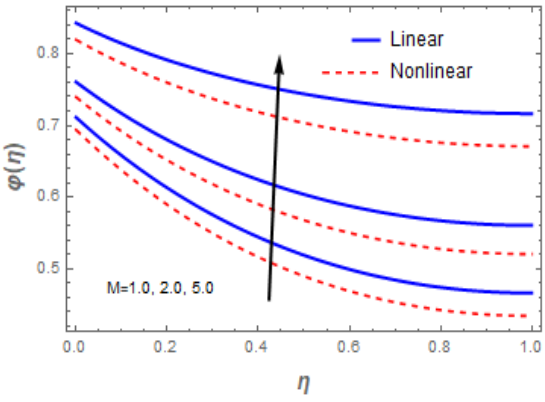

(c)

Fig. 2: The profiles of f', θ *and* φ for various values of M

The variation of the mixed convection parameter α_1 is seen on f', θ *and* φ in Figure 3 (a-c). Here,

it is examined that f' is increasing due to the presence of the buoyancy effect while θ *and* φ decay for larger values of α_1. The nonlinear α_1 has a greater influence on f', θ *and* φ than linear which signifies that the magnitude of buoyancy forces is more prevalent in the nonlinear case. The fluid horizontal velocity has the tendencies of approaching the free stream at the upper wall.

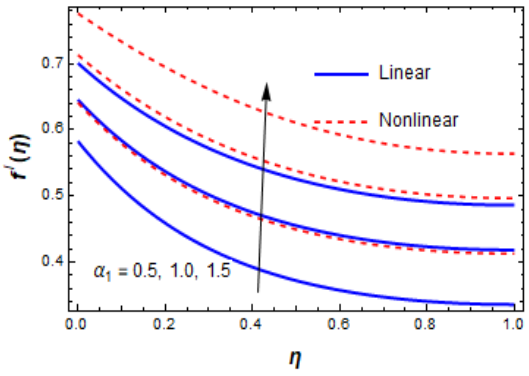

(a)

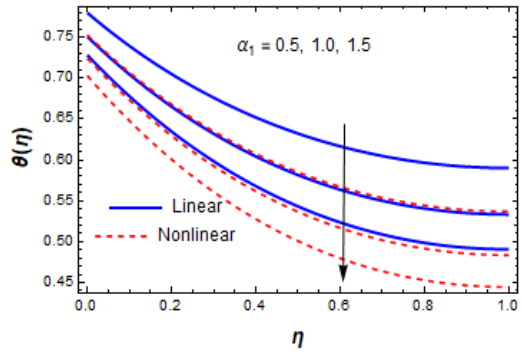

(b)

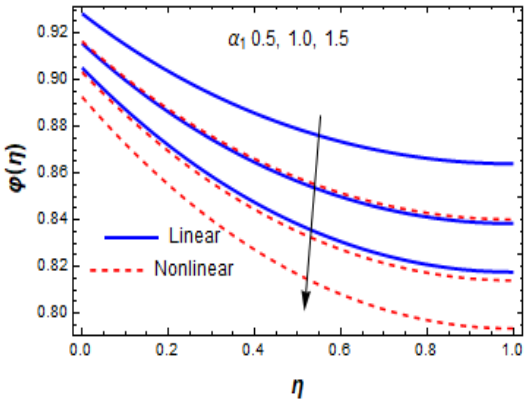

(c)

Fig. 3: The Profiles of f', θ *and* φ for various value of α_1

The influence of modified mixed convection f', θ *and* φ is elaborated in Figure 4 (a-c) respectively. The fluid velocity appreciates due to buoyancy force in Figure 4a while the temperature and concentration decelerate in Figure 4a and Figure b as α_3 improved. The nonlinear modified mixed convection α_3 has a significant effect on f', θ *and* φ on compared to linear case. Additionally, α_3 has a greater impact on the fluid variables to α_1.

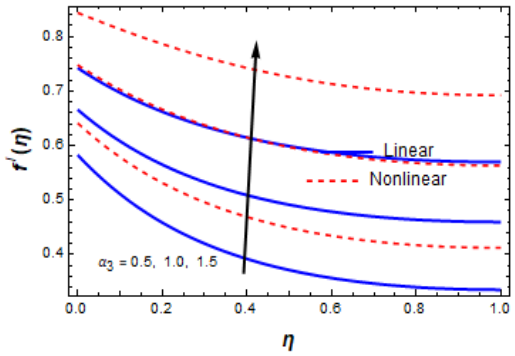

(a)

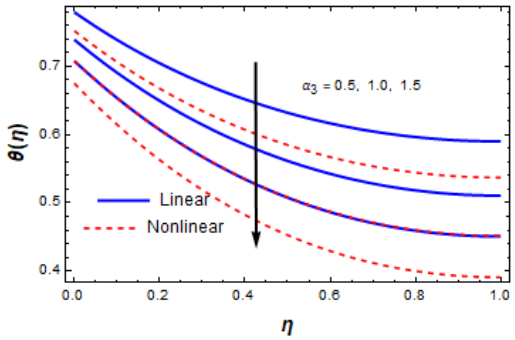

(b)

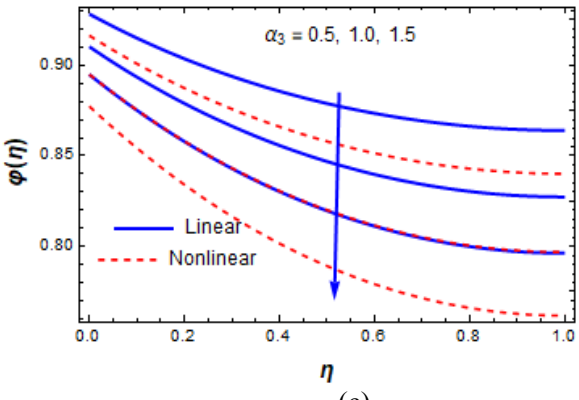

(c)

Fig. 4: The Profiles of f', θ *and* φ for various value of α_3

The significance of Pr on θ *and* φ is characterized in Figure 5 (a and b). The usefulness of Prandtl number in industrial activities to attain higher quality products can never be over-emphasized. Appropriate values of Pr are necessary in industrial heating/cooling. It is explored here that larger values of Prandtl number cause θ *and* φ to drop. Reduction in thermal diffusivity is the major characteristic in *Pr*. This factor resulted in the decrease of the thermal boundary layer and solutal concentration. Thus, Pr causes the fluid and solutal concentration to drop quicker in the nonlinear sense.

Figure 6 (a and b) portrays the rheological illustration of the profiles of θ *and* φ for improving values of Sc. It is explored that θ *and* φ lessens as Sc is enhanced due to the prevalent nature of the Brownian diffusion presence. The weak coefficient of Brownian diffusion signifies large values of Schmidt number which in turns lower the temperature profiles and solutal concentration. The Brownian diffusion's less prevalence in the presence of non-linear convection resulted in the fluid energy and concentration to drop faster compared to linear case.

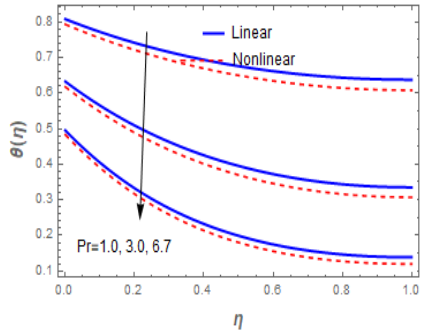

(a)

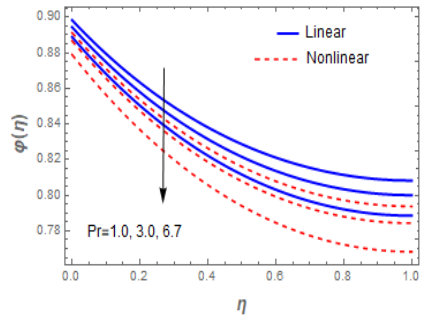

(b)

Fig. 5: The Profiles of θ and φ for various value of Pr

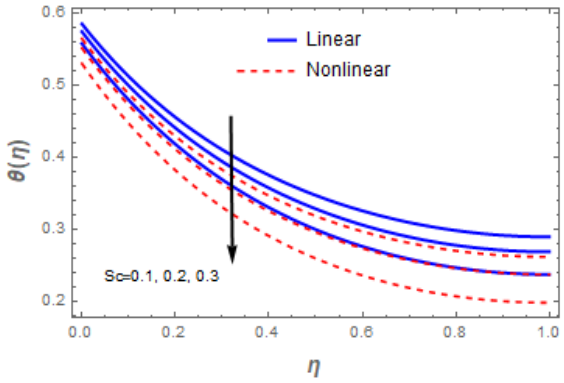

(a)

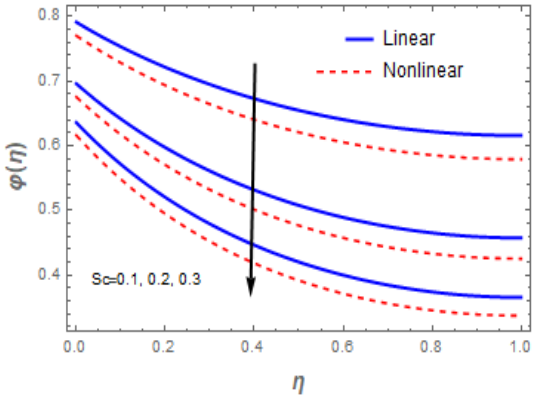

(b)

Fig. 6: The Profile of θ and φ for various values of Sc

Figure 7 (a-c) displays the impact of mixed convection and modified mixed convection α_1 *and* α_3 in the nonlinear sense on C_f, Nu_x, and Sh_x. Since the buoyancy parameters enhance the fluid velocity, the fluid particles gather momentum because of this enhancement causing more heat loss to the surrounding and thereby dropping the skin friction and increasing the Nusselt number and Sherwood number. This result agrees with, [48].

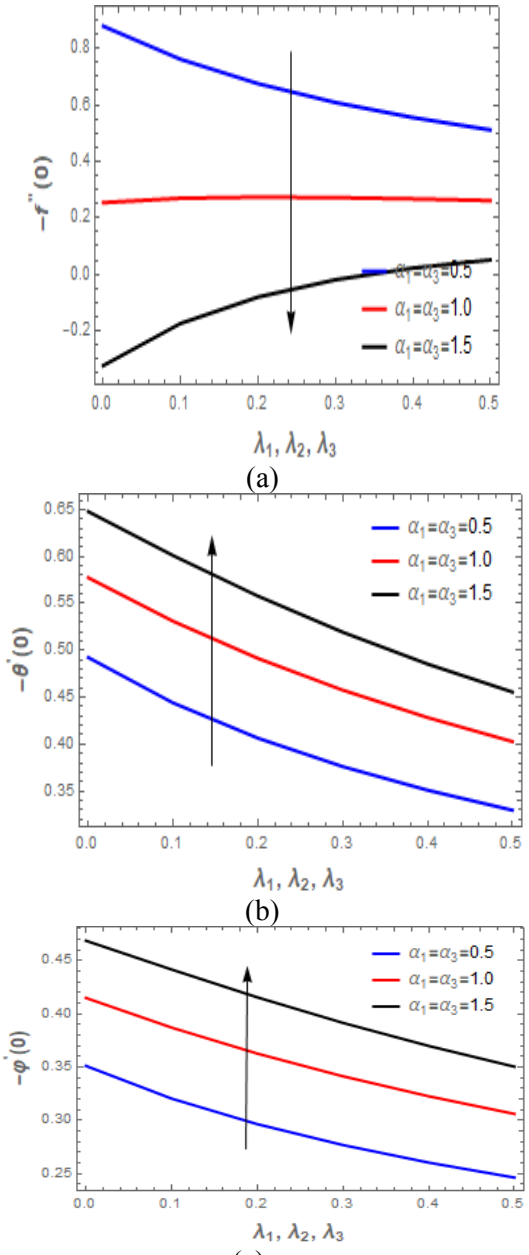

Fig. 7: The profiles of $-f''(0)$, $-\theta'(0)$, and $-\varphi'(0)$ for various values of α_1 and α_3

5 Conclusion

This study launched an investigation into the thermophysical properties of nonlinear/linear combined convective boundary layer slip-flow in a channel with a magnetic effect. Similarity solutions are introduced to transform the governing equation assisting the flow. Therefore, the solution to the nonlinear coupled set of ODE is numerically approximated using CCA. The approach gave an excellent result as illustrated in Table 1. In conclusion:

1. Magnetic parameters shrink the fluid momentum. Thus, the temperature and solutal concentration are enhanced.
2. The combined convective parameter and the modified mixed parameter have the same impact on the fluid variables. However, the modified mixed convection illustrates a greater impact.
3. Prandtl number Pr and Schmidt number Sc are reduction agents on the fluid energy and concentration.
4. Due to the influence slippery on the lower wall, the friction between the fluid and the wall surface drops with improve mixed and modified mixed convection. However, the Nusselt number and Sherwood number improved.

Interestingly, this analysis is significant in optimizing and modeling of Nonlinear combined convection in a horizontal channel with slip-flow regime rate of fluid material in each system. To improve the optimality of heat transfer conditions, nanofluids will be introduced in future work with slip-flow in a more complex geometry and the data will be trained using an ANN model to forecast the characteristics of heat and mass transfer.

References:

[1] N. Bachok, A. Ishak, I. Pop, Mixed Convection Boundary Layer Flow over a Moving Vertical Flat Plate in an External Fluid Flow with Viscous Dissipation Effect. *PLoS ONE* 8(4):e60766, 2013. https://doi.org/10.1371/journal.pone.0060766.

[2] N.A. Shah, C. Fetecau, D. Vieru, Natural convection flows of Prabhakar-like fractional Maxwell fluids with generalized thermal transport, *J. Therm. Anal. Calorim.* 143(3), 2021, p.2245–2258.

[3] K.M. Shirvan, M. Mamourian, S. Mirzakhanlari, A.B. Rahimi, R. Ellahi, Numerical study of surface radiation and combined natural convection heat transfer in a solar cavity receiver, *Int. J. Numer. Methods Heat Fluid Flow* 27, 2017, p.2385–2399.

[4] A. Ishak, Thermal boundary layer flow over a stretching sheet in a micropolar fluid with radiation effect, *Meccanica*. 45(3), 2010, p.367–373.

[5] Z. A. Khan, N. A. Shah, N. Haider, E. R. El-Zahar, S.J. Yook, Analysis of natural convection flows of Jeffrey fluid with Prabhakarlike thermal transport, *Case Stud. Therm. Eng*. 35, 2022, 102079.

[6] A.U. Rehman, F. Jarad, M.B. Riaz, Z.H. Shah, Generalized Mittag-leffler kernel form solutions of free convection heat and mass transfer flow of maxwell fluid with newtonian heating: Prabhakar fractional derivative approach, *Fractal Fract.* 6(2), 2022, p.98.

[7] K.V. Prasad, K. Vajravelu, P.S. Datti, Mixed convection heat transfer over a non-linear stretching surface with variable fluid properties, *Int. J. Non-Linear Mech.* 45(3), 2010, 320–330.

[8] S. Jena, G.C. Dash, S.R. Mishra, Chemical reaction effect on MHD viscoelastic fluid flow over a vertical stretching sheet with heat source/sink, *Ain Shams Eng. J.* 9(4), 2016, 1205–1213.

[9] T. Hayat, S. Qayyum, A. Alsaedi, B. Ahmad, Magnetohydrodynamic (MHD) nonlinear convective flow of Walters-B nanofluid over a nonlinear stretching sheet with variable thickness, *Int. J. Heat Mass Transf.* 110, 2017, 506–514.

[10] B. Mahanthesh, B.J. Gireesha, G.T. Thammanna, S.A. Shehzad, F.A. Abbasi, R. S. R. Gorla, Nonlinear convection in nano Maxwell fluid with nonlinear thermal radiation: A three-dimensional study, *Alexandria Engineering Journal* 57, 2018, 1927–1935. http://dx.doi.org/10.1016/j.aej.2017.03.037.

[11] M. A. Mansour, S. E. Ahmed, A.M. Rashad, MHD natural convection in a square enclosure using nanofluid with the influence of thermal boundary conditions, *Journal of Applied Fluid Mechanics* 9, 2016, 2515-2525.

[12] M. Tanveer, S. Ullah, N.A. Shah, Thermal analysis of free convection flows of viscous carbon nanotubes nanofluids with generalized thermal transport: A Prabhakar fractional model, *J. Therm. Anal. Calorim* 144(6), 2021, 2327–2336.

[13] S.A.A. Shah, N.A. Ahammad, B. Ali, K. Guedri, A.U. Awan, F. Gamaoun, E.M. Tag-ElDin, Significance of bio-convection, MHD, thermal radiation and activation energy across Prandtl nanofluid flow: A case of stretching cylinder, *Int. Commun. Heat Mass Transf.* 137, 2022, 106299.

[14] S.A.A. Shah, N.A. Ahammad, E.M. Tag-ElDin, F. Gamaoun, A.U. Awan, B. Ali, Bio-convection effects on Prandtl hybrid nanofluid flow with chemical reaction and motile microorganism over a stretching sheet, *Nanomaterials* 12(13), 2022, 174.

[15] A.U. Awan, S.A.A. Shah, B. Ali, Bio-convection effects on Williamson nanofluid flow with exponential heat source and motile microorganism over a stretching sheet. *Chin. J. Phys*.77, 2022, 2795–2810.

[16] A.U. Awan, S. Majeed, B. Ali, L. Ali, Significance of nanoparticles aggregation and Coriolis force on the dynamics of Prandtl nanofluid: The case of rotating flow, *Chin. J. Phys*. 79, 2022, 264–274.

[17] S.A.A. Shah, A.U. Awan, Significance of magnetized Darcy-Forchheimer stratified rotating Williamson hybrid nanofluid flow: A case of 3D sheet, *Int. Commun. Heat Mass Transf*. 136, 2022, 106214.

[18] M.V. Krishna, A.J. Chamkha, Hall and ion slip effects on MHD rotating boundary layer flow of nanofluid past an infinite vertical plate embedded in a porous medium, *Results in Physics* 15, 2019, 102652.

[19] M.V. Krishna, A.J. Chamkha, Hall effects on MHD squeezing flow of a water based nanofluid between two parallel disks, *Journal of Porous Media* 22, 2019, 209-223.

[20] M.V. Krishna, A.J. Chamkha, Hall and ion slip effects on unsteady MHD convective rotating flow of nanofluids-Application in Biomedical Engineering, *Journal of Egyptian Mathematical Society* 28, 2020, 1.

[21] U.R. Saif, M. Amna, U. Asmat, I.A. Muhammad, Y.B. Mohd, A.P. Bruno, A. Ali, Numerical computation of buoyancy and radiation effects on MHD micropolar nanofluid flow over a stretching/shrinking sheet with heat source, *Case Stud. Therm. Eng*. 25, 2021, 100867.

[22] C. Fetecau, I. Khan, F. Ali, S. Shafie, Radiation and porosity effects on the

magnetohydrodynamic flow past an oscillating vertical plate with uniform heat flux, *Z. für Naturforschung A*. 67, 2012, 572–580.

[23] M.V. Krishna, Heat transport on steady MHD flow of copper and alumina nanofluids past a stretching porous surface, *Heat Transfer* 49, 2020, 1374-1385.

[24] J. Singh, U.S. Mahabaleshwar, G. Bognar, Mass transpiration in nonlinear MHD flow due to porous stretching sheet, *Scientific Reports* 9, 2019, 1–15. https://doi.org/10.1038/s41598-019-52597-5 PMID: 31811160. Accessed 07/08/2023.

[25] J. Raza, A.M. Rohni, Z. Omar, Multiple solutions of mixed convective MHD Casson fluid flow in a channel, *Journal of Applied Mathematics (Hindawi Publishing Corporation)*, 7535793, 2016, p.1–10.

[26] U.S. Mahabaleshwar, I.E. Sarris, A.A. Hill, G. Lorenzini, I. Pop, An MHD couple stress fluid due to a perforated sheet undergoing linear stretching with heat transfer, *Int J Heat and Mass Trans*. 105, 2017, 157–167. https://doi.org/10.1016/j.ijheatmasstransfer.2016.09.040.

[27] U.S. Mahabaleshwar, K.R. Nagaraju, P.N.V. Kumar, N.A. Kelson, An MHD Navier's slip flow over axisymmetric linear stretching sheet using differential transform method, *Int J Appl Comput Math* 4(30), 2018, 1–13.

[28] J. Raza, Thermal radiation and slip effects on magnetohydrodynamic (MHD) stagnation point flow of Casson fluid over a convective stretching sheet, *Propulsion and Power Research* 8, 2019, 138–146. https://doi.org/10.1016/j.jppr.2019.01.004.

[29] M. Nazeer, F. Hussain, M.I. Khan, E.R. El-Zahar, Y.M. Chu, M. Malik, Theoretical study of MHD electroosmotically flow of third-grade fluid in microchannel, *Applied Mathematics and Computation* 420, 2022, 126868. https://doi.org/10.1016/j.amc.2021.126868.

[30] L.A. Lund, A. Omar, J. Raza, I. Khan, E.S.M. Sherif, Effects of stefan blowing and slip conditions on unsteady MHD Casson nanofluid flow over an unsteady shrinking sheet: dual solutions, *Symmetry* 12, 2020, 487. https://doi.org/10.3390/sym12030487.

[31] L. Zhang, M. Bhatti, E.E. Michaelides, M. Marin, R. Ellahi, Hybrid nanofluid flow towards an elastic surface with tantalum and nickel nanoparticles, under the influence of an induced magnetic field. *The European Physical Journal Special Topics*, 2021, p. 1–13.

[32] S.O. Salawu, H.A. Ogunseye, T.A. Yusuf, R.S. Lebelo, R.A. Mustapha, Entropy generation in a magnetohydrodynamic hybrid nanofluid flow over a nonlinear permeable surface with velocity slip effect. *WSEAS Transactions on Fluid Mechanics* 18, 2023, DOI: 10.37394/232013.2023.18.4.

[33] J. Chakraborty, S. Ray, S. Chakraborty, Role of streaming potential on pulsating mass flow rate control in combined electroosmotic and pressure-driven microfluidic devices, *Electrophoresis* 33, 2012, 419–425.

[34] B.K. Jha, M.O. Oni, Fully developed mixed convection flow in a vertical channel with electrokinetic effects: exact solution, *Multidiscipline Modeling in Materials and Structures* 14(5), 2018, 1031-1041. https://Doi.org/10.1108/MMMS-10-2017-0123.

[35] B.K. Jha, M.O. Oni, Mathematical modeling of combined pressure driven and electrokinetic effect in a channel with induced magnetic field: an exact solution, *J King Saud Univ Sci.* 31(4), 2018, 575-585. https://Doi.org/10.1016/j.jksus.2018.10.00910 18-3647.

[36] N.M.D. Khan, H. Xu, Q. Zhao, Q. Sun, Analysis of mixed convection in a vertical channel in the presence of electrical double layers, *Z Naturforsch* 73, 2018, 8. https ://Doi.org/10.1515/zna-2018-0097.

[37] B.K. Jha, M.O. Oni, Electromagnetic natural convection flow in a vertical microchannel with Joule heating: an exact solution, *J Taibah Univ Sci*. 12(5), 2018, 661-668. https ://Doi.org/10.1080/16583655.2018.1494423.

[38] B.K. Jha, M.O. Oni, B. Aina, Steady fully developed mixed convection flow in a vertical micro-concentric-annulus with heat generating/absorbing fluid: an exact solution, *Ain Shams Eng J.*, 2016. https://doi.org/10.1016/j.asej.2016.08.005.

[39] M. Safdar, K.M. Ijaz, R.A. Khan, S. Taj, F. Abbas, E. Samia, M.G. Ahmed, Analytic solutions for the MHD flow and heat transfer in a thin liquid film over an unsteady stretching surface with Lie symmetry and homotopy analysis method, *Waves in random and complex media* 33(2), 2023, 442–460. https://doi.org/10.1080/17455030.2022.2073402.

[40] K. Rakesh, S. Shilpa, Interaction of magnetic field and nonlinear convection in the stagnation point flow over a shrinking sheet, *Journal of Engineering*, 2016, 6752520. htttp://dx.doi.org/10.1155/2016/6752520.

[41] A.S. Idowu, M.T. Akolade, J.U. Abubakar, B.O. Falodun, MHD free convective heat and mass transfer flow of dissipative Casson fluid with variable viscosity and thermal conductivity effects, *Journal of Taibah University for Science* 14(1), 2020, 851-862.

[42] M.M. Babatin, Numerical treatment for the flow of Casson fluid and heat transfer model over an unsteady stretching surface in the presence of internal heat generation/absorption and thermal radiation, *Applications & Applied Mathematics* 13(2), 2018, 854-862.

[43] T. Javed, I. Mustafa, Slip effect on a mixed convection flow of a third-grade fluid near the orthogonal stagnation point on a vertical surface, *Journal of Applied Mechanics and Technical Physics* 57(3), 2016 527-536.

[44] F. Mallawi, Application of a legendre collocation method to the space time variable fractional-order advection dispersion equation, *J. Taibah Univ. Sci*.13(1), 2019, 324-330.

[45] L.J. Grubka, K.M. Bobba, Heat transfer characteristics of a continuous stretching surface with variable temperature, *J. Heat Transfer* 107, 1985, 248-250.

[46] I.C. Liu, A note on heat and mass transfer for a hydromagnetic flow over a stretching sheet, *Int. Commun. Heat mass Transfer* 32, 2005, 1075-1084.

[47] A. Ishaq, Unsteady MHD flow and heat transfer over a stretching plate, *J. Appl. Sci*. 10(18), 2010, 2127-2131.

[48] A.I. Fagbade, B.O. Falodun, A.J. Omowaye, MHD natural convection flow of viscoelastic fluid over an accelerating permeable surface with thermal radiation and heat source or sink: Spectral Homotopy Analysis Approach, *Ain Shams Engineering Journal* 9, 2018, 1029–1041. http://dx.doi.org/10.1016/j.asej.2016.04.021.

Contribution of Individual Authors to the Creation of a Scientific Article (Ghostwriting Policy)

The authors equally contributed to the present research, at all stages from the formulation of the problem to the final findings and solution.

Sources of Funding for Research Presented in a Scientific Article or Scientific Article Itself

No funding was received for conducting this study.

Conflict of interest

The authors have no conflicts of interest to declare.

Nomenclature

t	Time (s)	α_3	Modified mixed convective parameter $(=Gc_x/\mathrm{Re}_x^2)$
a_1, a_2, a_3	Slip constants	α_4	Nonlinear solutal buoyancy parameter $(=\beta_3(T_0-T_h)/\beta_2)$
k	Thermal conductivity (W/mK)	Pr	Prandtl number $(=\upsilon/\alpha^*)$
$h(t)$	Wall distance $(=\beta\sqrt{\upsilon(1-\alpha t)/b})$ (m)	Sc	Schmidt number υ/D_M
g	Acceleration due to gravity (m/s^2)	λ_1	Velocity slip parameter $(=(a_1/\beta)\sqrt{b/\upsilon(1-\alpha t)})$
T	Fluid temperature (K)	λ_2	Temperature slip parameter $(=(a_2/\beta)\sqrt{b/\upsilon(1-\alpha t)})$
x, y	Fluid directions (m)	λ_3	Concentration slip parameter $(=(a_3/\beta)\sqrt{b/\upsilon(1-\alpha t)})$
u, v	Fluid velocities along (m/s) x, y	C_f	Coefficient of skin friction
b	Stretching constant (-)	Nu_x	Coefficient of Nusselt number
T_0	Fluid temperature at lower wall (K)	Sh_x	Coefficient of Sherwood number
T_h	Fluid temperature at upper wall (K)	D_1	Temperature difference $(=(T_0-T_h)/x)$ (K)
C	Fluid concentration (kg/m^3)	D_2	Solutal difference $(=(C_0-C_h)/x)$ (kg/m^3)
C_o	Fluid concentration at the lower wall (kg/m^3)		*Greek Symbols*
C_h	Fluid concentration at upper wall(kg/m^3)	η	Fluid dimensionless distance (m)
f	Fluid dimensionless Velocity m/s	α, β	Squeezing characteristic parameters (-)
s	Dimensionless measure of unsteadiness $(=\alpha/b)$	υ	Kinematic viscousity (m^2s^{-1})
M	Magnetic parameter ($=\sigma B_0^2/\rho$)	θ	Dimensionless temperature
Gt_x	Thermal Grashof number $(=g\beta_0(T_0-T_h)x^3/\upsilon^2)$	φ	Dimensionless concentration
Gc_x	Solutal Grashof number $(=g\beta_2(C_0-C_h)x^3/\upsilon^2)$	ρ	Fluid density (kgm^{-3})
γ	Squeezing parameter $(=\beta^2)$	σ	Electrical conductivity
Re_x	Reanold number $(=bx^2/(1-\alpha t)\upsilon)$	β_0, β_1	Coefficient of thermal expansion
α_1	Mixed convective parameter $(=Gt_x/\mathrm{Re}_x^2)$	β_2, β_3	Coefficient of solutal expansion

α_2	Nonlinear thermal buoyancy parameter $(=\beta_1(T_0-T_h)/\beta_0)$	*Superscript*	
B	Magnetic effect $B_0/\sqrt{1-\alpha t}$	'	Derivative with respect to η
u_0	Stretching value $(=bx/(1-\alpha t))$	α^*	Thermal diffusivity
D_M	Molecular Diffusion		